Semi-supervised semantic segmentation needs strong, varied perturbations

Geoff French[1]
g.french@uea.ac.uk
Samuli Laine[2]
slaine@nvidia.com
Timo Aila[2]
taila@nvidia.com
Michal Mackiewicz[1]
m.mackiewicz@uea.ac.uk
Graham aFinalyson[1]
g.finlayson@uea.ac.uk

[1] School of Computing Sciences
University of East Anglia
Norwich, UK
[2] NVIDIA
Helsinki, Finland

Abstract

Consistency regularization describes a class of approaches that have yielded ground breaking results in semi-supervised classification problems. Prior work has established the cluster assumption — under which the data distribution consists of uniform class clusters of samples separated by low density regions — as important to its success. We analyse the problem of semantic segmentation and find that its' distribution does not exhibit low density regions separating classes and offer this as an explanation for why semi-supervised segmentation is a challenging problem, with only a few reports of success. We then identify choice of augmentation as key to obtaining reliable performance without such low-density regions. We find that adapted variants of the recently proposed CutOut and CutMix augmentation techniques yield state-of-the-art semi-supervised semantic segmentation results in standard datasets. Furthermore, given its challenging nature we propose that semantic segmentation acts as an effective *acid test* for evaluating semi-supervised regularizers. Implementation at: https://github.com/Britefury/cutmix-semisup-seg.

1 Introduction

Semi-supervised learning offers the tantalizing promise of training a machine learning model using datasets that have labels for only a fraction of their samples. These situations often arise in practical computer vision problems where large quantities of images are readily available and ground truth annotation acts as a bottleneck due to the cost and labour required.

Consistency regularization [19, 25, 26, 32] describes a class of semi-supervised learning algorithms that have yielded state-of-the-art results in semi-supervised classification, while being conceptually simple and often easy to implement. The key idea is to encourage the network to give consistent predictions for unlabelled inputs that are perturbed in various ways.

The effectiveness of consistency regularization is often attributed to the *smoothness assumption* [23] or *cluster assumption* [6, 31, 33, 37]. The smoothness assumption states that samples close to each other are likely to have the same label. The cluster assumption — a special case of the smoothness assumption — states that decision surfaces should lie in low density regions of the data distribution. This typically holds in classification tasks, where most successes of consistency regularization have been reported so far.

At a high level, semantic segmentation is classification, where each pixel is classified based on its neighbourhood. It is therefore intriguing that there are only two reports of consistency regularization being successfully applied to segmentation from the medical imaging community [21, 28] and none for natural photographic images. We make the observation that the L^2 pixel content distance between patches centred on neighbouring pixels varies smoothly even when the class of the centre pixel changes, and thus there are no low-density regions along class boundaries. This alarming observation leads us to investigate the conditions that can allow consistency regularization to operate in these circumstances.

We find mask-based augmentation strategies to be effective for semi-supervised semantic segmentation, with an adapted variant of CutMix [39] realizing significant gains.

The key contributions of our paper are our analysis of the data distribution of semantic segmentation and the simplicity of our approach. We utilize tried and tested semi-supervised learning approaches, and adapt CutMix – an augmentation technique for supervised classification – for semi-supervised learning and for segmentation, achieving state of the art results.

2 Background

Our work relates to prior art in three areas: recent regularization techniques for classification, semi-supervised classification with a focus on consistency regularization, and semantic segmentation.

2.1 MixUp, Cutout, and CutMix

The MixUp regularizer of Zhang *et al.* [40] improves the performance of supervised image, speech and tabular data classifiers by using interpolated samples during training. The inputs and target labels of two randomly chosen examples are blended using a randomly chosen factor.

The Cutout regularizer of Devries *et al.* [11] augments an image by masking a rectangular region to zero. The recently proposed CutMix regularizer of Yun *et al.* [39] combines aspects of MixUp and CutOut, cutting a rectangular region from image B and pasting it over image A. MixUp, Cutout, and CutMix improve supervised classification performance, with CutMix outperforming the other two.

2.2 Semi-supervised classification

A wide variety of consistency regularization based semi-supervised classification approaches have been proposed in the literature. They normally combine a standard supervised loss term (e.g. cross-entropy loss) with an unsupervised consistency loss term that encourages consistent predictions in response to perturbations applied to unsupervised samples.

The Π-model of Laine *et al.* [19] passes each unlabelled sample through a classifier twice, applying two realizations of a stochastic augmentation process, and minimizes the squared difference between the resulting class probability predictions. Their temporal model and the model of Sajjadi *et al.* [32] encourage consistency between the current and historical predictions. Miyato *et al.* [25] replaced the stochastic augmentation with adversarial directions, thus aiming perturbations toward the decision boundary.

The mean teacher model of Tarvainen *et al.* [36] encourages consistency between predictions of a student network and a teacher network whose weights are an exponential moving average [29] of those of the student. Mean teacher was used for domain adaptation in [13].

The Unsupervised data augmentation (UDA) model [38] and the state of the art FixMatch model [34] demonstrate the benefit of rich data augmentation as both combine CutOut [11] with RandAugment [10] (UDA) or CTAugment [3] (FixMatch). RandAugment and CTAugment draw from a repertoire of 14 image augmentations.

Interpolation consistency training (ICT) of Verma *et al.* [37] and MixMatch [4] both combine MixUp [40] with consistency regularization. ICT uses the mean teacher model and applies MixUp to unsupervised samples, blending input images along with teacher class predictions to produce a blended input and target to train the student.

2.3 Semantic segmentation

Most semantic segmentation networks transform an image classifier into a fully convolutional network that produces a dense set of predictions for overlapping input windows, segmenting input images of arbitrary size [22]. The DeepLab v3 [7] architecture increases localization accuracy by combining atrous convolutions with spatial pyramid pooling. Encoder-decoder networks [2, 20, 30] use skip connections to connect an image classifier like encoder to a decoder. The encoder down-samples the input progressively, while the decoder up-samples, producing an output whose resolution natively matches the input.

A number of approaches for semi-supervised semantic segmentation use additional data. Kalluri *et al.* [17] use data from two datasets from different domains, maximizing the similarity between per-class embeddings from each dataset. Stekovic *et al.* [35] use depth images and enforced geometric constraints between multiple views of a 3D scene.

Relatively few approaches operate in a strictly semi-supervised setting. Hung *et al.* [16] and Mittal *et al.* [24] employ GAN-based adversarial learning, using a discriminator network that distinguishes real from predicted segmentation maps to guide learning.

The only successful applications of consistency regularisation to segmentation that we are aware of come from the medical imaging community; Perone *et al.* [28] and Li *et al.* [21] apply consistency regularization to an MRI volume dataset and to skin lesions respectively. Both approaches use standard augmentation to provide perturbation.

3 Consistency regularization for semantic segmentation

Consistency regularization adds a consistency loss term L_{cons} to the loss that is minimized during training [26]. In a classification task, L_{cons} measures a distance $d(\cdot,\cdot)$ between the predictions resulting from applying a neural network f_θ to an unsupervised sample x and a perturbed version $\hat{x}$ of the same sample, i.e., $L_{cons} = d(f_\theta(x), f_\theta(\hat{x}))$. The perturbation used to generate $\hat{x}$ depends on the variant of consistency regularization used. A variety of distance measures $d(\cdot,\cdot)$ have been used, e.g., squared distance [19] or cross-entropy [25].

The benefit of the cluster assumption is supported by the formal analysis of Athiwaratkun *et al.* [1]. They analyse a simplified Π-model [19] that uses additive isotropic Gaussian noise

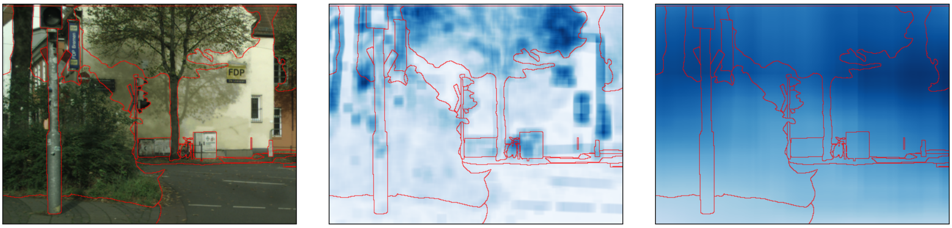

(a) Example image (b) Avg. distance to neighbour, patch size 15×15 (c) Avg. distance to neighbour, patch size 225×225

Figure 1: In a segmentation task, low-density regions rarely correspond to class boundaries. (a) An image crop from the CITYSCAPES dataset. (b) Average L^2 distance between raw pixel contents of a patch centred at pixel p and four overlapping patches centred on the immediate neighbours of p, using 15×15 pixel patches. (c) Same for a more realistic receptive field size of 225×225 pixels. A darker colour indicates larger inter-patch distance and therefore a low density region. Red lines indicate segmentation ground truth boundaries.

for perturbation ($\hat{x} = x + \varepsilon\mathcal{N}(0,1)$) and find that the expected value of L_{cons} is approximately proportional to the squared magnitude of the Jacobian $J_{f_\theta}(x)$ of the networks outputs with respect to its inputs. Minimizing L_{cons} therefore flattens the decision function in the vicinity of unsupervised samples, moving the decision boundary — and its surrounding region of high gradient — into regions of low sample density.

3.1 Why semi-supervised semantic segmentation is challenging

We view semantic segmentation as sliding window patch classification with the goal of identifying the class of the patch's central pixel. Given that prior works [19, 25, 34] apply perturbations to the raw pixel (input) space our analysis of the data distribution focuses on the raw pixel content of image patches, rather than higher level features from within the network.

We attribute the infrequent success of consistency regularization in natural image semantic segmentation problems to the observations that low density regions in input data do not align well with class boundaries. The presence of such low density regions would manifest as locally larger than average L^2 distances between patches centred on neighbouring pixels that lie either side of a class boundary. In Figure 1 we visualise the L^2 distances between neighbouring patches. When using a reasonable receptive field as in Figure 1 (c) we can see that the cluster assumption is clearly violated: how much the raw pixel content of the receptive field of one pixel differs from the contents of the receptive field of a neighbouring pixel has little correlation with whether the patches' centre pixels belong to the same class.

The lack of variation in the patchwise distances is easy to explain from a signal processing perspective. With patch of size $H \times W$, the distance map of L^2 distances between the pixel content of overlapping patches centred on all pairs of horizontally neighbouring pixels can be written as $\sqrt{(\Delta_{\mathrm{x}} I)^{\circ 2} * 1^{H\times W}}$, where $*$ denotes convolution and $\Delta_{\mathrm{x}} I$ is the horizontal gradient of the input image I. The element-wise squared gradient image is thus low-pass filtered by a $H \times W$ box filter[1], which suppresses the fine details found in the high frequency components of the image, leading to smoothly varying sample density across the image.

Our analysis of the CITYSCAPES dataset quantifies the challenges involved in placing a decision boundary between two neighbouring pixels that should belong to different classes,

[1] We explain our derivation in our supplemental material

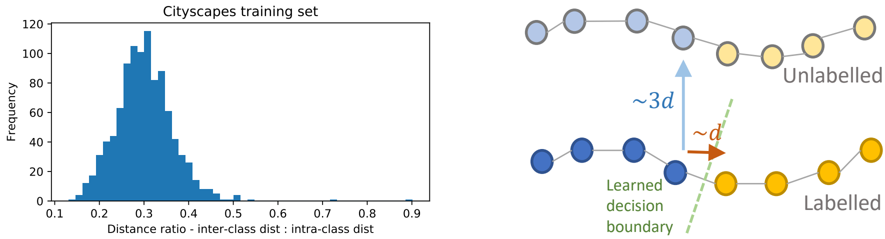

Figure 2: **Left:** histogram of the ratio $|N_i - A_i|^2 / |P_i - A_i|^2$ of the L_2 pixel content inter-class distance between patches A_i and N_i centred on neighbouring pixels either side of class boundary to the intra-class distance between nearest neighbour patches A_i and P_i coming from different images. **Right:** conceptual illustration of semantic segmentation sample distribution. The chain of samples (circles) below represents a row of patches from an image changing class (colour) half-way through. The lighter chain above represents an unlabelled image. The dashed green line represents a learned decision boundary. The samples within an image are at a distance of $\sim d$ from one another and $\sim 3d$ from those in another image.

while generalizing to other images. We find that the L^2 distance between patches centred on pixels on either side of a class boundary is $\sim 1/3$ of the distance to the closest patch of the same class found in a different image (see Figure 2). This suggests that precise positioning and orientation of the decision boundary are essential for good performance. We discuss our analysis in further detail in our supplemental material.

3.2 Consistency regularization without the cluster assumption

When considered in the context of our analysis above, the few reports of the successful application of consistency regularization to semantic segmentation – in particular the work of Li *et al.* [21] – lead us to conclude that the presence of low density regions separating classes is highly beneficial, but not essential. We therefore suggest an alternative mechanism: that of using non-isotropic natural perturbations such as image augmentation to constrain the orientation of the decision boundary to lie parallel to the directions of perturbation (see the appendix of Athiwaratkun *et al.* [1]). We will now explore this using a 2D toy example.

Figure 3a illustrates the benefit of the cluster assumption with a simple 2D toy mean teacher experiment, in which the cluster assumption holds due to the presence of a gap separating the unsupervised samples that belong to two different classes. The perturbation used for L_{cons} is an isotropic Gaussian nudge to both coordinates, and as expected, the learned decision boundary settles neatly between the two clusters. In Figure 3b the unsupervised samples are uniformly distributed and the cluster assumption is violated. In this case, the consistency loss does more harm than good; even though it successfully flattens the neighbourhood of the decision function, it does so also across the true class boundary.

In Figure 3c, we plot the contours of the distance to the true class boundary. If we constrain the perturbation applied to a sample x such that the perturbed $\hat{x}$ lies on or very close to the distance contour passing through x, the resulting learned decision boundary aligns well with the true class boundary, as seen in Figure 3d. When low density regions are not present the perturbations must be carefully chosen such that the probability of crossing the class boundary is minimised.

We propose that reliable semi-supervised segmentation is achievable provided that the

Isotropic perturbation | Constrained perturbation

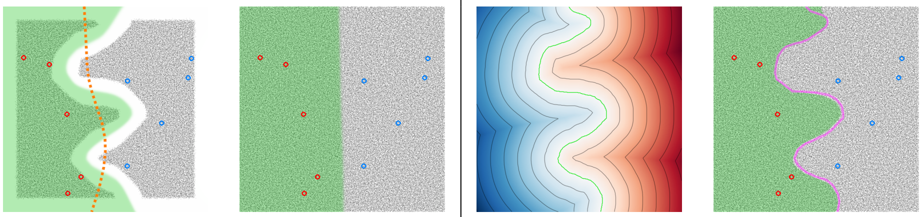

(a) Low density region separating classes (b) No low density region (c) Distance map and contours (d) Constrain to dist. map contours

Figure 3: Toy 2D semi-supervised classification experiments. Blue and red circles indicate supervised samples from class 0 and 1 respectively. The field of small black dots indicate unsupervised samples. The learned decision function is visualized by rendering the probability of class 1 in green. (a, b) Semi-supervised learning with and without a low density region separating the classes. The dotted orange line in (a) shows the decision boundary obtained with plain supervised learning. (c) Rendering of the distance to the true class boundary with distance map contours. Strong colours indicate greater distance to class boundary. (d) Decision boundary learned when samples are perturbed along distance contours in (c). The magenta line indicates the true class boundary.

augmentation/perturbation mechanism observes the following guidelines: 1) the perturbations must be varied and high-dimensional in order to sufficiently constrain the orientation of the decision boundary in the high-dimensional space of natural imagery, 2) the probability of a perturbation crossing the true class boundary must be very small compared to the amount of exploration in other dimensions, and 3) the perturbed inputs should be plausible; they should not be grossly outside the manifold of real inputs.

Classic augmentation based perturbations such as cropping, scaling, rotation and colour changes have a low chance of confusing the output class and have proved to be effective in classifying natural images [19, 36]. Given that this approach has positive results in some medical image segmentation problems [21, 28], it is surprising that it is ineffective for natural imagery. This motivates us to search for stronger and more varied augmentations for semi-supervised semantic segmentation.

3.3 CutOut and CutMix for semantic segmentation

Cutout [11] yielded strong results in semi-supervised classification in UDA [38] and FixMatch [34]. The UDA ablation study shows Cutout contributing the lions share of the semi-supervised performance, while the FixMatch ablation shows that CutOut can match the effect of the combination of 14 image operations used by CTAugment. DeVries *et al.* [11] established that Cutout encourages the network to utilise a wider variety of features in order to overcome the varying combinations of parts of an image being present or masked out. This variety introduced by Cutout suggests that it is a promising candidate for segmentation.

As stated in Section 2.1, CutMix combines Cutout with MixUp, using a rectangular mask to blend input images. Given that MixUp has been successfully used in semi-supervised classification in ICT [37] and MixMatch [4], we propose using CutMix to blend unsupervised samples and corresponding predictions in a similar fashion.

Preliminary experiments comparing the Π-model [19] and the mean teacher model [36] indicate that using mean teacher is essential for good performance in semantic segmentation, therefore all the experiments in this paper use the mean teacher framework. We denote the student network as f_θ and the teacher network as g_ϕ.

Cutout. As in [11] we initialize a mask M with the value 1 and set the pixels inside a randomly chosen rectangle to 0. To apply Cutout in a semantic segmentation task, we mask the input pixels with M and disregard the consistency loss for pixels masked to 0 by M. FixMatch [34] uses a *weak* augmentation scheme consisting of crops and flips to predict pseudo-labels used as targets for samples augmented using the *strong* CTAugment scheme. Similarly, we consider Cutout to be a form of *strong* augmentation, so we apply the teacher network g_ϕ to the original image to generate pseudo-targets that are used to train the student f_θ. Using square distance as the metric, we have $L_{cons} = ||M \odot (f_\theta(M \odot x) - g_\phi(x))||^2$, where $\odot$ denotes an element-wise product.

CutMix. CutMix requires two input images that we shall denote x_a and x_b that we mix with the mask M. Following ICT ([37]) we mix the teacher predictions for the input images $g_\phi(x_a), g_\phi(x_b)$ producing a pseudo target for the student prediction of the mixed image. To simplify the notation, let us define function $mix(a,b,M) = (1-M) \odot a + M \odot b$ that selects the output pixel based on mask M. We can now write the consistency loss as:

$$L_{cons} = \left|\left| mix\Big(g_\phi(x_a), g_\phi(x_b), M\Big) - f_\theta\Big(mix(x_a, x_b, M)\Big) \right|\right|^2. \tag{1}$$

The original formulation of Cutout [11] for classification used a rectangle of a fixed size and aspect ratio whose centre was positioned randomly, allowing part of the rectangle to lie outside the bounds of the image. CutMix [39] randomly varied the size, but used a fixed aspect ratio. For segmentation we obtained better performance with CutOut by randomly choosing the size and aspect ratio and positioning the rectangle so it lies entirely within the image. In contrast, CutMix performance was maximized by fixing the area of the rectangle to half that of the image, while varying the aspect ratio and position.

While the augmentations applied by Cutout and CutMix do not appear in real-life imagery, they are reasonable from a visual standpoint. Segmentation networks are frequently trained using image crops rather than full images, so blocking out a section of the image with Cutout can be seen as the inverse operation. Applying CutMix in effect pastes a rectangular region from one image onto another, similarly resulting in a reasonable segmentation task.

Cutout and CutMix based consistency loss are illustrated in our supplemental material.

4 Experiments

We will now describe our experiments and main results. We will start by describing the training setup, followed by results on the PASCAL VOC 2012, CITYSCAPES and ISIC 2017 datasets. We compare various perturbation methods in the context of semi-supervised semantic segmentation on PASCAL and ISIC.

4.1 Training setup

We use two segmentation networks in our experiments: 1) DeepLab v2 network [6] based on ImageNet pre-trained ResNet-101 as used in [24] and 2) Dense U-net [20] based on DensetNet-161 [15] as used in [21]. We also evaluate using DeepLab v3+ [8] and PSPNet [41] in our supplemental material.

We use cross-entropy for the supervised loss L_{sup} and compute the consistency loss L_{cons} using the Mean teacher algorithm [36]. Summing L_{cons} over the class dimension and averaging over others allows us to minimize L_{sup} and L_{cons} with equal weighting. Further details and hyper-parameter settings are provided in supplemental material. We replace the sigmoidal ramp-up that modulates L_{cons} in [19, 36] with the average of the thresholded confidence of the teacher network, which increases as the training progresses [13, 18, 34].

4.2 Results on Cityscapes and Augmented Pascal VOC

Here we present our results on two natural image datasets and contrast them against the state-of-the-art in semi-supervised semantic segmentation, which is currently the adversarial training approach of Mittal *et al.* [24]. We use two natural image datasets in our experiments. CITYSCAPES consists of urban scenery and has 2975 images in its training set. PASCAL VOC 2012[12] is more varied, but includes only 1464 training images, and thus we follow the lead of Hung *et al.* [16] and augment it using SEMANTIC BOUNDARIES[14], resulting in 10582 training images. We adopted the same cropping and augmentation schemes as [24].

In addition to an ImageNet pre-trained DeepLab v2, Hung [16] and Mittal *et al.* [24] also used a DeepLabv2 network pre-trained for semantic segmentation on the COCO dataset, whose natural image content is similar to that of PASCAL. Their results confirm the benefits of task-specific pre-training. Starting from a pre-trained ImageNet classifier is representative of practical problems for which a similar segmentation dataset is unavailable for pre-training, so we opted to use these more challenging conditions only.

Our CITYSCAPES results are presented in Table 1 as mean intersection-over-union (mIoU) percentages, where higher is better. Our supervised baseline results for CITYSCAPES are similar to those of [24]. We attribute the small differences to training regime choices such as the choice of optimizer. Both the Cutout and CutMix realize improvements over the supervised baseline, with CutMix taking the lead and improving on the adversarial[16] and s4GAN[24] approaches. We note that CutMix performance is slightly impaired when full size image crops are used getting an mIoU score of $58.75\% \pm 0.75$ for 372 labelled images. Using a mixing mask consisting of three smaller boxes – see supplemental material – whose scale better matches the image content alleviates this, obtaining $60.41\% \pm 1.12$.

Our PASCAL results are presented in Table 2. Our baselines are considerably weaker than those of [24]; we acknowledge that we were unable to match them. Cutout and CutMix yield improvements over our baseline and CutMix – in spite of the weak baseline – takes the lead, ahead of the adversarial and s4GAN results. Virtual adversarial training [25] yields a noticeable improvement, but is unable to match competing approaches. The improvement obtained from ICT [37] is just noticeable, while standard augmentation makes barely any difference. Please see our supplemental material for results using DeepLab v3+ [8] and PSPNet [41] networks.

4.3 Results on ISIC 2017

The ISIC skin lesion segmentation dataset [9] consists of dermoscopy images focused on lesions set against skin. It has 2000 images in its training set and is a two-class (skin and lesion) segmentation problem, featuring far less variation than CITYSCAPES and PASCAL.

We follow the pre-processing and augmentation schemes of Li *et al.* [21]; all images were scaled to 248×248 and our augmentation scheme consists of random 224×224 crops, flips, rotations and uniform scaling in the range 0.9 to 1.1.

Labeled samples	~1/30 (100)	1/8 (372)	1/4 (744)	All (2975)
	Results from [16, 24] with ImageNet pre-trained DeepLab v2			
Baseline	—	56.2%	60.2%	66.0%
Adversarial [16]	—	57.1%	60.5%	66.2%
s4GAN [24]	—	59.3%	61.9%	65.8%
	Our results: Same ImageNet pre-trained DeepLab v2 network			
Baseline	44.41% ± 1.11	55.25% ± 0.66	60.57% ± 1.13	67.53% ± 0.35
Cutout	47.21% ± 1.74	57.72% ± 0.83	61.96% ± 0.99	67.47% ± 0.68
CutMix	**51.20% ± 2.29**	**60.34% ± 1.24**	**63.87% ± 0.71**	**67.68% ± 0.37**

Table 1: Performance (mIoU) on CITYSCAPES validation set, presented as mean ± std-dev computed from 5 runs. The results for [16] and [24] are taken from [24].

Labeled samples	1/100	1/50	1/20	1/8	All (10582)
	Results from [16, 24] with ImageNet pre-trained DeepLab v2				
Baseline	–	48.3%	56.8%	62.0%	70.7%
Adversarial [16]	–	49.2%	59.1%	64.3%	71.4%
s4GAN+MLMT [24]	–	60.4%	62.9%	67.3%	**73.2%**
	Our results: Same ImageNet pre-trained DeepLab v2 network				
Baseline	33.09%	43.15%	52.05%	60.56%	72.59%
Std. augmentation	32.40%	42.81%	53.37%	60.66%	72.24%
VAT	38.81%	48.55%	58.50%	62.93%	72.18%
ICT	35.82%	46.28%	53.17%	59.63%	71.50%
CutOut	48.73%	58.26%	64.37%	66.79%	72.03%
CutMix	**53.79%**	**64.81%**	**66.48%**	**67.60%**	72.54%

Table 2: Performance (mIoU) on augmented PASCAL VOC validation set, using same splits as Mittal *et al.* [24]. The results for [16] and [24] are taken from [24].

We present our results in Table 3. We must first note that our supervised baseline results are noticeably worse that those of Li *et al.* [21]. Given this limitation, we use our results to contrast the effects of the different augmentation schemes used. Our strongest semi-supervised result was obtained using CutMix, followed by standard augmentation, then VAT and CutOut. We found CutMix to be the most reliable, as the other approaches required more hyper-parameter tuning effort to obtain positive results. We were unable to obtain reliable performance from ICT, hence its result is worse than that of the baseline.

We propose that the good performance of standard augmentation – in contrast to PASCAL where it makes barely any difference – is due to the lack of variation in the dataset. An augmented variant of an unsupervised sample is sufficient similar to other samples in the dataset to successfully propagate labels, in spite of the limited variation introduced by standard augmentation.

4.4 Discussion

We initially hypothesized that the strong performance of CutMix on the CITYSCAPES and PASCAL datasets was due to the augmentation in effect 'simulating occlusion', exposing the network to a wider variety of occlusions, thereby improving performance on natural images.

Baseline	Std. aug.	VAT	ICT	Cutout	CutMix	Fully sup.
Results from [21] with ImageNet pre-trained DenseUNet-161						
72.85%	**75.31%**	–	–	–	–	79.60%
Our results: ImageNet pre-trained DenseUNet-161						
67.64%	71.40%	69.09%	65.45%	68.76%	**74.57%**	78.61%
$\pm$1.83	$\pm$2.34	$\pm$1.38	$\pm$3.50	$\pm$4.30	$\pm$**1.03**	$\pm$0.36

Table 3: Performance on ISIC 2017 skin lesion segmentation validation set, measured using the Jaccard index (IoU for lesion class). Presented as mean $\pm$ std-dev computed from 5 runs. All baseline and semi-supervised results use 50 supervised samples. The fully supervised result ('Fully sup.') uses all 2000.

This was our motivation for using the ISIC 2017 dataset; its' images do not feature occlusions and soft edges delineate lesions from skin[27]. The strong performance of CutMix indicates that the presence of occlusions is not a requirement.

The success of virtual adversarial training demonstrates that exploring the space of adversarial examples provides sufficient variation to act as an effective semi-supervised regularizer in the challenging conditions posed by semantic segmentation. In contrast the small improvements obtained from ICT and the barely noticeable difference made by standard augmentation on the PASCAL dataset indicates that these approaches are not suitable for this domain; we recommend using a more varied source or perturbation, such as CutMix.

5 Conclusions

We have demonstrated that consistency regularization is a viable solution for semi-supervised semantic segmentation, provided that an appropriate source of augmentation is used. Its data distribution lacks low-density regions between classes, hampering the effectiveness of augmentation schemes such as affine transformations and ICT. We demonstrated that richer approaches can be successful, and presented an adapted CutMix regularizer that provides sufficiently varied perturbation to enable state-of-the-art results and work reliably on natural image datasets. Our approach is considerably easier to implement and use than the previous methods based on GAN-style training.

We hypothesize that other problem domains that involve segmenting continuous signals given sliding-window input – such as audio processing – are likely to have similarly challenging distributions. This suggests mask-based regularization as a potential avenue.

Finally, we propose that the challenging nature of the data distribution present in semantic segmentation indicates that it is an effective *acid test* for evaluating future semi-supervised regularizers.

Acknowledgements

Part of this work was done during an internship at nVidia. This work was in part funded under the European Union Horizon 2020 SMARTFISH project, grant agreement no. 773521. Much of the computation required by this work was performed on the University of East Anglia HPC Cluster. We would like to thank Jimmy Cross, Amjad Sayed and Leo Earl. We would like thank nVidia corporation for their generous donation of a Titan X GPU.

References

[1] Ben Athiwaratkun, Marc Finzi, Pavel Izmailov, and Andrew Gordon Wilson. There are many consistent explanations of unlabeled data: Why you should average. In *International Conference on Learning Representations*, 2019.

[2] Vijay Badrinarayanan, Alex Kendall, and Roberto Cipolla. Segnet: A deep convolutional encoder-decoder architecture for image segmentation. *CoRR*, abs/1511.00561, 2015.

[3] David Berthelot, Nicholas Carlini, Ekin D Cubuk, Alex Kurakin, Kihyuk Sohn, Han Zhang, and Colin Raffel. Remixmatch: Semi-supervised learning with distribution alignment and augmentation anchoring. *arXiv preprint arXiv:1911.09785*, 2019.

[4] David Berthelot, Nicholas Carlini, Ian Goodfellow, Nicolas Papernot, Avital Oliver, and Colin Raffel. Mixmatch: A holistic approach to semi-supervised learning. *CoRR*, abs/1905.02249, 2019.

[5] Olivier Chapelle and Alexander Zien. Semi-supervised classification by low density separation. In *AISTATS*, volume 2005, pages 57–64, 2005.

[6] Liang-Chieh Chen, George Papandreou, Iasonas Kokkinos, Kevin Murphy, and Alan L Yuille. Deeplab: Semantic image segmentation with deep convolutional nets, atrous convolution, and fully connected CRFs. *IEEE transactions on pattern analysis and machine intelligence*, 40(4):834–848, 2017.

[7] Liang-Chieh Chen, George Papandreou, Florian Schroff, and Hartwig Adam. Rethinking atrous convolution for semantic image segmentation. *arXiv preprint arXiv:1706.05587*, 2017.

[8] Liang-Chieh Chen, Yukun Zhu, George Papandreou, Florian Schroff, and Hartwig Adam. Encoder-decoder with atrous separable convolution for semantic image segmentation. In *Proceedings of the European conference on computer vision (ECCV)*, pages 801–818, 2018.

[9] Noel CF Codella, David Gutman, M Emre Celebi, Brian Helba, Michael A Marchetti, Stephen W Dusza, Aadi Kalloo, Konstantinos Liopyris, Nabin Mishra, Harald Kittler, et al. Skin lesion analysis toward melanoma detection: A challenge at the 2017 international symposium on biomedical imaging (isbi), hosted by the international skin imaging collaboration (isic). In *2018 IEEE 15th International Symposium on Biomedical Imaging (ISBI 2018)*, pages 168–172. IEEE, 2018.

[10] Ekin D Cubuk, Barret Zoph, Jonathon Shlens, and Quoc V Le. Randaugment: Practical data augmentation with no separate search. *arXiv preprint arXiv:1909.13719*, 2019.

[11] Terrance DeVries and Graham W Taylor. Improved regularization of convolutional neural networks with cutout. *CoRR*, abs/1708.04552, 2017.

[12] M. Everingham, L. Van Gool, C. K. I. Williams, J. Winn, and A. Zisserman. The PASCAL Visual Object Classes Challenge 2012 (VOC2012) Results, 2012.

[13] Geoff French, Michal Mackiewicz, and Mark Fisher. Self-ensembling for visual domain adaptation. In *International Conference on Learning Representations*, 2018.

[14] Bharath Hariharan, Pablo Arbeláez, Lubomir Bourdev, Subhransu Maji, and Jitendra Malik. Semantic contours from inverse detectors. In *International Conference on Computer Vision*, pages 991–998, 2011.

[15] Gao Huang, Zhuang Liu, Laurens Van Der Maaten, and Kilian Q Weinberger. Densely connected convolutional networks. In *Proceedings of the IEEE conference on computer vision and pattern recognition*, pages 4700–4708, 2017.

[16] Wei-Chih Hung, Yi-Hsuan Tsai, Yan-Ting Liou, Yen-Yu Lin, and Ming-Hsuan Yang. Adversarial learning for semi-supervised semantic segmentation. *CoRR*, abs/1802.07934, 2018.

[17] Tarun Kalluri, Girish Varma, Manmohan Chandraker, and CV Jawahar. Universal semi-supervised semantic segmentation. *CoRR*, abs/1811.10323, 2018.

[18] Zhanghan Ke, Daoye Wang, Qiong Yan, Jimmy Ren, and Rynson WH Lau. Dual student: Breaking the limits of the teacher in semi-supervised learning. In *Proceedings of the IEEE International Conference on Computer Vision*, pages 6728–6736, 2019.

[19] Samuli Laine and Timo Aila. Temporal ensembling for semi-supervised learning. In *International Conference on Learning Representations*, 2017.

[20] Xiaomeng Li, Hao Chen, Xiaojuan Qi, Qi Dou, Chi-Wing Fu, and Pheng-Ann Heng. H-denseunet: hybrid densely connected unet for liver and tumor segmentation from ct volumes. *IEEE transactions on medical imaging*, 37(12):2663–2674, 2018.

[21] Xiaomeng Li, Lequan Yu, Hao Chen, Chi-Wing Fu, and Pheng-Ann Heng. Semi-supervised skin lesion segmentation via transformation consistent self-ensembling model. In *British Machine Vision Conference*, 2018.

[22] Jonathan Long, Evan Shelhamer, and Trevor Darrell. Fully convolutional networks for semantic segmentation. In *IEEE Conference on Computer Vision and Pattern Recognition*, pages 3431–3440, 2015.

[23] Yucen Luo, Jun Zhu, Mengxi Li, Yong Ren, and Bo Zhang. Smooth neighbors on teacher graphs for semi-supervised learning. In *IEEE Conference on Computer Vision and Pattern Recognition*, pages 8896–8905, 2018.

[24] Sudhanshu Mittal, Maxim Tatarchenko, and Thomas Brox. Semi-supervised semantic segmentation with high-and low-level consistency. *IEEE Transactions on Pattern Analysis and Machine Intelligence*, 2019.

[25] Takeru Miyato, Schi-ichi Maeda, Masanori Koyama, and Shin Ishii. Virtual adversarial training: a regularization method for supervised and semi-supervised learning. *arXiv preprint arXiv:1704.03976*, 2017.

[26] Avital Oliver, Augustus Odena, Colin Raffel, Ekin D. Cubuk, and Ian J. Goodfellow. Realistic evaluation of semi-supervised learning algorithms. In *International Conference on Learning Representations*, 2018.

[27] Fábio Perez, Cristina Vasconcelos, Sandra Avila, and Eduardo Valle. Data augmentation for skin lesion analysis. In *OR 2.0 Context-Aware Operating Theaters, Computer Assisted Robotic Endoscopy, Clinical Image-Based Procedures, and Skin Image Analysis*, pages 303–311. Springer, 2018.

[28] Christian S Perone and Julien Cohen-Adad. Deep semi-supervised segmentation with weight-averaged consistency targets. In *Deep Learning in Medical Image Analysis and Multimodal Learning for Clinical Decision Support*, pages 12–19. Springer, 2018.

[29] Boris T Polyak and Anatoli B Juditsky. Acceleration of stochastic approximation by averaging. *SIAM Journal on Control and Optimization*, 30(4):838–855, 1992.

[30] Olaf Ronneberger, Philipp Fischer, and Thomas Brox. U-net: Convolutional networks for biomedical image segmentation. In *International Conference on Medical Image Computing and Computer-Assisted Intervention*, pages 234–241, 2015.

[31] Mehdi Sajjadi, Mehran Javanmardi, and Tolga Tasdizen. Mutual exclusivity loss for semi-supervised deep learning. In *23rd IEEE International Conference on Image Processing, ICIP 2016*, 2016.

[32] Mehdi Sajjadi, Mehran Javanmardi, and Tolga Tasdizen. Regularization with stochastic transformations and perturbations for deep semi-supervised learning. In *Advances in Neural Information Processing Systems*, pages 1163–1171, 2016.

[33] Rui Shu, Hung Bui, Hirokazu Narui, and Stefano Ermon. A DIRT-t approach to unsupervised domain adaptation. In *International Conference on Learning Representations*, 2018.

[34] Kihyuk Sohn, David Berthelot, Chun-Liang Li, Zizhao Zhang, Nicholas Carlini, Ekin D Cubuk, Alex Kurakin, Han Zhang, and Colin Raffel. Fixmatch: Simplifying semi-supervised learning with consistency and confidence. *arXiv preprint arXiv:2001.07685*, 2020.

[35] Sinisa Stekovic, Friedrich Fraundorfer, and Vincent Lepetit. S4-net: Geometry-consistent semi-supervised semantic segmentation. *CoRR*, abs/1812.10717, 2018.

[36] Antti Tarvainen and Harri Valpola. Mean teachers are better role models: Weight-averaged consistency targets improve semi-supervised deep learning results. In *Advances in Neural Information Processing Systems*, pages 1195–1204, 2017.

[37] Vikas Verma, Alex Lamb, Juho Kannala, Yoshua Bengio, and David Lopez-Paz. Interpolation consistency training for semi-supervised learning. *CoRR*, abs/1903.03825, 2019.

[38] Qizhe Xie, Zihang Dai, Eduard Hovy, Minh-Thang Luong, and Quoc V Le. Unsupervised data augmentation. *arXiv preprint arXiv:1904.12848*, 2019.

[39] Sangdoo Yun, Dongyoon Han, Seong Joon Oh, Sanghyuk Chun, Junsuk Choe, and Youngjoon Yoo. Cutmix: Regularization strategy to train strong classifiers with localizable features. In *Proceedings of the IEEE International Conference on Computer Vision*, pages 6023–6032, 2019.

[40] Hongyi Zhang, Moustapha Cisse, Yann N. Dauphin, and David Lopez-Paz. mixup: Beyond empirical risk minimization. In *International Conference on Learning Representations*, 2018.

[41] Hengshuang Zhao, Jianping Shi, Xiaojuan Qi, Xiaogang Wang, and Jiaya Jia. Pyramid scene parsing network. In *Proceedings of the IEEE conference on computer vision and pattern recognition*, pages 2881–2890, 2017.